MICHIGAN STATE UNIVERSITY

CYCLOTRON PROJECT*

Magnetic Coil Design for a Superconducting Air-Cored 40 Mev Cyclotron

Richard Berg

January 1963

Department of Physics

East Lansing, Michigan

---

*Research Supported in part by The National Science Foundation (Grant NSF-G19978)

ABSTRACT

MAGNETIC COIL DESIGN FOR A SUPERCONDUCTING
AIR-CORED 40-MEV CYCLOTRON

by Richard Berg

Recently discovered hard superconductors open the possibility of constructing iron-free particle accelerators of various types. Medium energy cyclotrons appear to be particularly suited to initial application of the technique since the field is fixed and the magnets are of moderate size. As an aid in assessing the feasibility of such a device the physical configuration of the coil network was calculated. The resulting coils are appealingly simple. In addition, in order to obtain an initial acquaintance with pertinent technical problems, a small super-conducting Nb-Zr solenoid was constructed and operated.

MAGNETIC COIL DESIGN FOR A SUPERCONDUCTING AIR-CORED 40-MEV CYCLOTRON

By

Richard Berg

A THESIS

Submitted to
Michigan State University
in partial fulfillment of the requirements
for the degree of

MASTER OF SCIENCE

Department of Physics and Astronomy

1963

ACKNOWLEDGMENTS

I should like to thank Dr. H. G. Blosser for suggesting the problem and for his help during the course of the work, and Dr. R. D. Spence for his helpful suggestions concerning the low temperature work.

I should also like to thank Julie Wescott for her help with the drawings.

Finally, I am grateful to the National Science Foundation for financial support of the work.

TABLE OF CONTENTS

LIST OF TABLES

LIST OF FIGURES

Figure

INTRODUCTION

The conventional cyclotron, developed in the early 1930's by E. O. Lawrence and associates, has significant energy limitations due to conflicting requirements placed on the magnetic field: 1) to achieve focusing, the field must decrease with radius, and 2) for relativistic particles to retain constant orbital angular velocities, the field must increase with radius as the mass of the particle. Thus, for the conventional cyclotron, the attainment of moderately relativistic particles is impractical unless one modulates the radio frequency dee voltage, as in the synchrocyclotron, a process which severely limits the current output.

In 1938, L. H. Thomas demonstrated the practicability of a fixed frequency relativistic cyclotron,[1] by showing that one could obtain additional focusing through the introduction of an azimuthally-varying field, thus eliminating the necessity of the first of the above requirements. Cyclotrons of this general type are usually called sector-focused, or Fixed-Field-Alternating-Gradient (FFAG), cyclotrons.

Due to a substantial increase in the design complication, no attempt was made to construct a sectored cyclotron

for over a decade.[2] Nearly two decades elapsed before the idea took full flower in the late 1950's with efforts undertaken at a number of institutions to construct machines in the medium energy range. At the present time there are roughly half a dozen operating FFAG cyclotrons in the world, and several others in various stages of design or construction.[3] Most of the new cyclotrons now under construction or design are sectored, and plans to convert several other conventional cyclotrons to the sectored type have been made.

Studies thus far have shown sectored cyclotrons to have superior focusing properties, while at the same time retaining the high output current of the conventional fixed-frequency cyclotron. This is achieved while producing relativistic particles not possible with the conventional machine.

Nevertheless, many of the problems met with the conventional cyclotron are still present in the sectored cyclotron. The magnitude of the magnetic field is limited by the permeability of the iron, and the size of the pole tips is limited in many cases by the amount of iron necessary and its related cost. Further, the design of the pole tips is quite involved due to the complicated behavior of iron in high magnetic fields.

The phenomenon of superconductivity, whereby the

electrical resistance of a substance becomes identically zero at temperatures near absolute zero, was discovered in 1911 by Heike Kamerlingh Onnes.[4] Since that time, superconductivity has been discovered in many elements, compounds, and alloys. Ensuing investigation has also disclosed that for each superconducting substance there are critical values of temperature, magnetic field, and current density, above which the superconductivity ceases. These three critical values are found to depend upon each other as well as upon the type of material involved.

For many years most of the known superconducting substances were in a class called "soft" superconductors, characterized in general by physical softness, very low critical temperatures, and low critical magnetic fields and current densities. The current in a soft superconductor is carried primarily in the thin shell at the surface of the wire. More recently, a class of "hard" superconductors has been discovered,[5] being generally characterized by physical hardness and brittleness, higher critical temperatures, and extremely high critical magnetic fields and current densities. In a hard superconductor the current is believed to be transported by filaments which are evenly distributed throughout the wire. The number of these filaments can be increased by physically working the wire before it is cooled.

An example of the "hard" superconductors is the alloy Niobium-25% Zirconium, which was used in the work described. Its critical temperature is greater than 10°K, and the critical current density is more than 20,000 amperes per square centimeter in fields of 50,000 gauss.[6] Although it is very hard, and tends to be brittle, it is quite workable if one exercises a certain amount of care.

One significant outgrowth of the recent discovery and investigation of the hard superconductors has been the increasing ease with which very high magnetic fields may be produced. Superconducting magnets have been suggested[7] and are commercially available[8] for lasers, masers, Mössbauer experiments, and NMR experiments, and further consideration suggests their adaptability to cyclotrons as well.

Such a cyclotron would have several advantages. Its field would not be limited to the traditional 20 kilogauss maximum of iron, but by the critical field of the superconducting substance used. The practical size limitations could be relaxed since the weight of the machine would be significantly reduced. Design procedure could be immensely simplified; most of the design work could be done by computation alone, without recourse to model magnets, and without the necessity of dealing with the peculiarities of odd-shaped iron pole pieces. Even with refrigeration power included, the

total power consumption of the machine should decrease significantly.

Of course, there are problems involved with this type of machine also, the most significant of which seem to be the cost of the superconducting material and the details concerning the low temperature bath. It is likely, however, that in the near future physicists will develop materials which will become superconducting at substantially higher temperatures, and, hopefully, that some day the art of producing these superconducting materials will be advanced to the point where they may be made less expensively. It is quite probable that the reduction in power consumed by a superconducting magnet system will more than compensate for the additional cost of materials and cooling.

The objective of this work is to indicate the feasibility of construcing such a superconducting magnet for a medium energy cyclotron using Nb-25% Zr alloy. Thin wire approximations are first used to calculate a workable field. From this the cross-sectional area of wire bundles needed to produce the field without exceeding the critical current density is derived and a final network of coils developed. The calculated orbits of particles in this field show stability up to the various extraction energies, and the placement of

the resulting wire loops indicates a very convenient arrangement of coils may be obtained.

UNITS AND DEFINITIONS

For this thesis, the usual right cylindrical polar coordinate system is used, with the origin at the geometrical center of the magnetic field. The axial reference plane is the "median plane," i.e., the plane of symmetry of the magnetic field. The magnetic field on the median plane is strictly axial, and can be given by a Fourier series:

$$B_z(r,\theta) = \overline{B}(r) + \sum_n \left(H_{nN}(r) \cos n N\theta + G_{nN}(r) \sin n N\theta\right)$$

where N is the number of sectors. For small values of Z, the axial component of the magnetic field remains approximately constant, and the radial and azimuthal components can be calculated by expanding the median plane field in a Taylor series:

$$B_r(r,\theta,Z) \simeq Z \frac{\partial B_z(r,\theta)}{\partial r}$$

$$B_\theta(r,\theta,Z) \simeq \frac{Z}{r} \frac{\partial B_z(r,\theta)}{\partial \theta}$$

As a convenience in the numerical calculations, a set of dimensionless, relativistic units well suited to cyclotron work, called "cyclotron units," is employed.[9] Fundamental quantities are taken to be the rest mass m_o, the speed of light c, and the charge q. If the angular frequency

ω_{rf} of the radio-frequency accelerating voltage is arbitrarily chosen, the magnetic field unit B_o is then given by

$$B_o = \frac{m_o c}{q} \omega_{rf}$$

and the unit of time is then given by

$$\tau_o = \frac{1}{\omega_{rf}}.$$

The cyclotron length unit is then defined:

$$a = \frac{c}{\omega_{rf}}.$$

All quantities are then given as ratios to the appropriate cyclotron units: energies in units of the rest energy $m_o c^2$, momenta in units of $m_o c$, lengths in units of a, magnetic field in units of B_o, frequencies in units of ω_{rf}.

For any energy, the equilibrium orbit is defined as the median plane orbit which returns to its original coordinates in radial phase space (r, p_r) after one sector.

Radial and axial betatron oscillations are the small oscillatory deviations of the trajectory of the particle about its equilibrium orbit. The small amplitude radial and axial focusing frequencies are defined respectively as the ratio of the radial and axial betatron oscillation frequency to the particle angular frequency:

$$\nu_r = \frac{\omega_r}{\omega_{rf}}, \quad \nu_z = \frac{\omega_z}{\omega_{r_f}}.$$

If particles of all energies have a constant rotation period, the field is isochronous.

COMPUTER PROGRAMS

Several computer programs were used regularly throughout the course of the work. A magnetic field routine was written which calculates the field of an arbitrary series of thin straight wire segments by evaluating the Biot-Savart expression.[10] Another routine calculates the off-axis field of a circular turn of thin wire by evaluating the elliptic integrals numerically with a rapidly converging iteration.[11] Most of the field fitting was done with a least squares computer routine, which considers the coil data as the coefficients of a set of simultaneous linear equations, and numerically calculates the best solutions.[12] A Fourier series routine was used to make a harmonic analysis of the flutter field.[13] An equilibrium orbit program integrates the equations of motion in the median plane to find the radial phase space co-ordinates of the equilibrium orbits at $\theta = 0^{o}$ as a function of energy.[14] This program also gives the average radius and orbital frequency of the particle in this orbit and its small amplitude radial and axial focusing frequencies. Isochronous average fields were calculated in a two-part sequence: given a first

approximation of the isochronous field, and the flutter field, a second approximation was calculated; then, using this field and the equilibrium orbits obtained in it, a more refined approximation was made.[15] Other programs were helpful in various phases of the numerical work.

DESIGN PROCEDURE

To design a set of coils producing fields capable of giving the proper characteristics to an accelerating beam of any of the desired particles, the following general procedure was adopted. First, as indicated in detail below, an ideal combination of flutter and average fields was found. The ideal flutter was then matched with a proposed set of flutter coils. For preliminary design, a fictitious particle whose mass increase (and therefore whose increase in isochronous average field) lay between that of the light and heavy particles was chosen. The isochronous average field for the proposed flutter field was calculated, and was then matched by a group of chosen circular coils in a sequence of least square fits. The coils chosen by this procedure could then be used to produce an adequate field for any of the several particles.

In developing an appropriate ideal combination of flutter and average fields, three general requirements were placed on the equilibrium orbits: 1) the orbits must be isochronous to one part per thousand, i.e., the phase slip per turn cannot exceed this limit, 2) the axial focusing

frequency ν_z must be approximately equal to 0.2, within about 25% tolerance, 3) the radial focusing frequence ν_r must be greater than one over the range of acceleration, passing through the $\nu_r = 1$ resonance at the extraction energy. Further, ν_r and ν_z must remain approximately constant until near the extraction energy in order that other resonances do not occur.

Approximate relations may be obtained between the equilibrium orbit parameters and the fields and their derivatives.[16] In the circular orbit approximation (i.e., field increasing with radius, no azimuthal variation) the isochronous average field is given by

$$B(r) = \frac{B_o}{\sqrt{1 - r^2/a^2}} \tag{1}$$

where B_o is the central field, r is the radius, and a is the cyclotron length unit. First approximations of the axial and radial focusing frequencies are given by the "smooth approximation"[17]:

$$\nu_z^2 = -k + F, \tag{2}$$

$$\nu_r^2 = 1 + k, \tag{3}$$

for strictly radial sectors (no spiral).

Here k is the field index defined by

$$k = \frac{r}{\bar{B}} \frac{d\bar{B}}{dr} \tag{4}$$

where $\overline{B}$ is the average field as a function of radius:

$$\overline{B}(r) = \frac{1}{2\pi} \int_0^{2\pi} B\,(r,\theta)\, d\theta. \tag{5}$$

F is the flutter function defined by

$$F(r) = \frac{\langle [B(r,\theta) - \overline{B}(r)]^2 \rangle}{\overline{B}^2(r)}. \tag{6}$$

Using the flutter field in the calculations, a more accurate approximation for the isochronous average field is[18]

$$\langle B \rangle = B_o \frac{1 + \frac{F}{2N^2}}{(1-\beta(r)^2)^{1/2} \left(1 + \frac{1}{4N^2} \left[6F + 2r \frac{dF}{dr} \right] \right)} \tag{7}$$

where N is the number of sectors, and

$$\beta(r) = \frac{r}{a} \left(1 + \frac{F}{2N^2} \right). \tag{8}$$

The equations for isochronous average field, ν_r, and ν_z are coupled, with the result that specification of isochronism and either ν_r or ν_z essentially determines the other. In the present case it was desired to obtain an isochronous field with $\nu_z = 0.2 \pm 25\%$, as specified above. To find the ideal field to produce such orbit characteristics an iteration process was used. A first approximation of the isochronous average field was calculated from equation (1). Using this, the flutter needed to give $\nu_z = 0.2$ was

calculated by equation (2), and this in turn used in equation (7) to find a better isochronous average field. Equations (2) and (7) were then used in succession to obtain a combination of average and flutter fields in which the parameters of the equilibrium orbits converged to the desired values. The smooth approximation $\langle B \rangle$ and the resulting $\langle B \rangle$ and flutter after the iteration converged are shown in Figure 1 as a function of radius. Table 1 shows the properties of typical equilibrium orbits in such an ideal field obtained from the computer. The values of the functions listed are observed to fall within the specifications which were given.

Since the circular coils produce no azimuthal variation, the design problem is simplified if the sector coils are first designed such as to produce the desired flutter as nearly as possible. With this flutter field, the appropriate isochronous average field can then be produced by a set of circular coils.

Since the desired coil design was to be such as to render the cyclotron capable of accelerating several types of ions, preliminary design of the coils was carried through using the fictitious particle previously referred to; the relativistic mass increase of this particle and hence the rate of increase of the average field, lies midway between that of the proton and the heavy ions. After carrying through

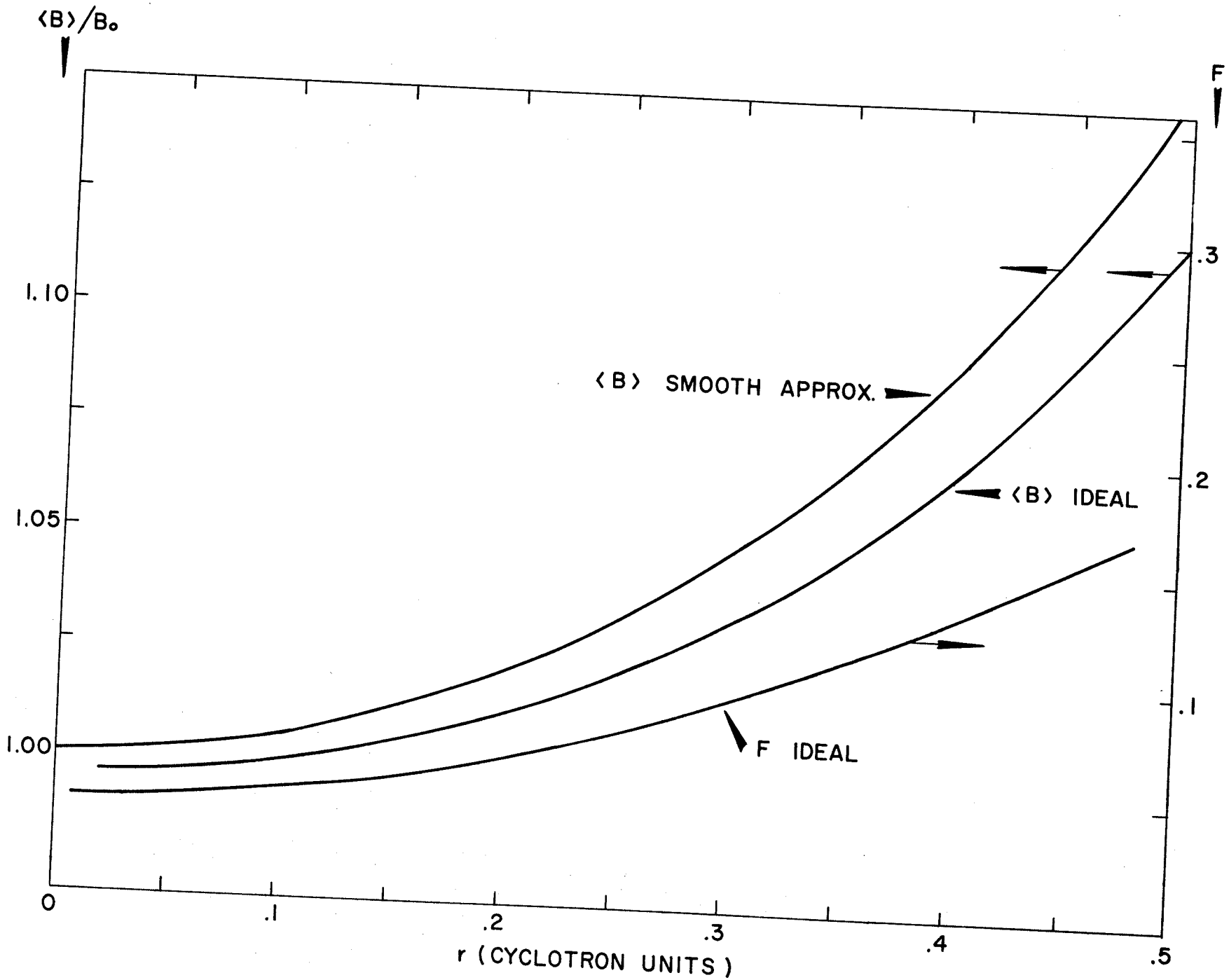

Fig. 1: Smooth approximation isochronous average field; ideal $\nu_z = 0.2$ flutter and its isochronous average field.

Table 1. Equilibrium orbits in an isochronous, ν_z = 0.2 field produced by iteration of equations (2) and (7).

00000000000 10 HEX RK +0050000000 +9382300

E	R AV	PHASE	R	PR	NU R	NU Z
+00800	+12930460	-00007913	+13443274	-00000002	+10286198	+02025789
+01600	+18158790	-00014680	+18944398	-00000002	+10443215	+01917013
+02400	+22086321	-00021697	+23113818	-00000003	+10603742	+01800503
+03200	+25328620	-00030027	+26582430	-00000003	+10765883	+01691049
+04000	+28126200	-00039991	+29595821	-00000003	+10938329	+01506979

the preliminary design, a set of coils resulted which could readily be programmed for fields with slightly lower or slightly higher average field gradient.

A symmetric kite-shaped turn as shown in Figure 2 was chosen for the sector coil. The total flutter field is produced by six of these turns, three at 120° spacing above the median plane, and three in a mirror image below the median plane. The cyclotron magnetic field thus consisted of three strictly radial sectors. The dimensions indicated in Figure 2 are in cyclotron units, a particle at the extraction energy having an average radius of approximately 0.20, in these units.

The field of a flutter coil was calculated at a polar grid of points on the median plane, using 48 angle values at each radius, and a radial spacing of 0.005 cyclotron units, which yields forty radius values at which the field is stored out to the extraction radius. Having the field of a single coil, the total symmetric flutter field of the six coils was synthesized.

Choosing $\theta = 0^{\circ}$ at the center of one of the loops as in Figure 2, a Fourier analysis of the field at each radius was performed, and the field expressed in the form

$$B(r,\theta) = \overline{B}(r) + \sum_{n=1}^{3} \left(H_{3n}(r) \cos 3n\theta + G_{3n}(r) \sin 3n\theta \right).$$

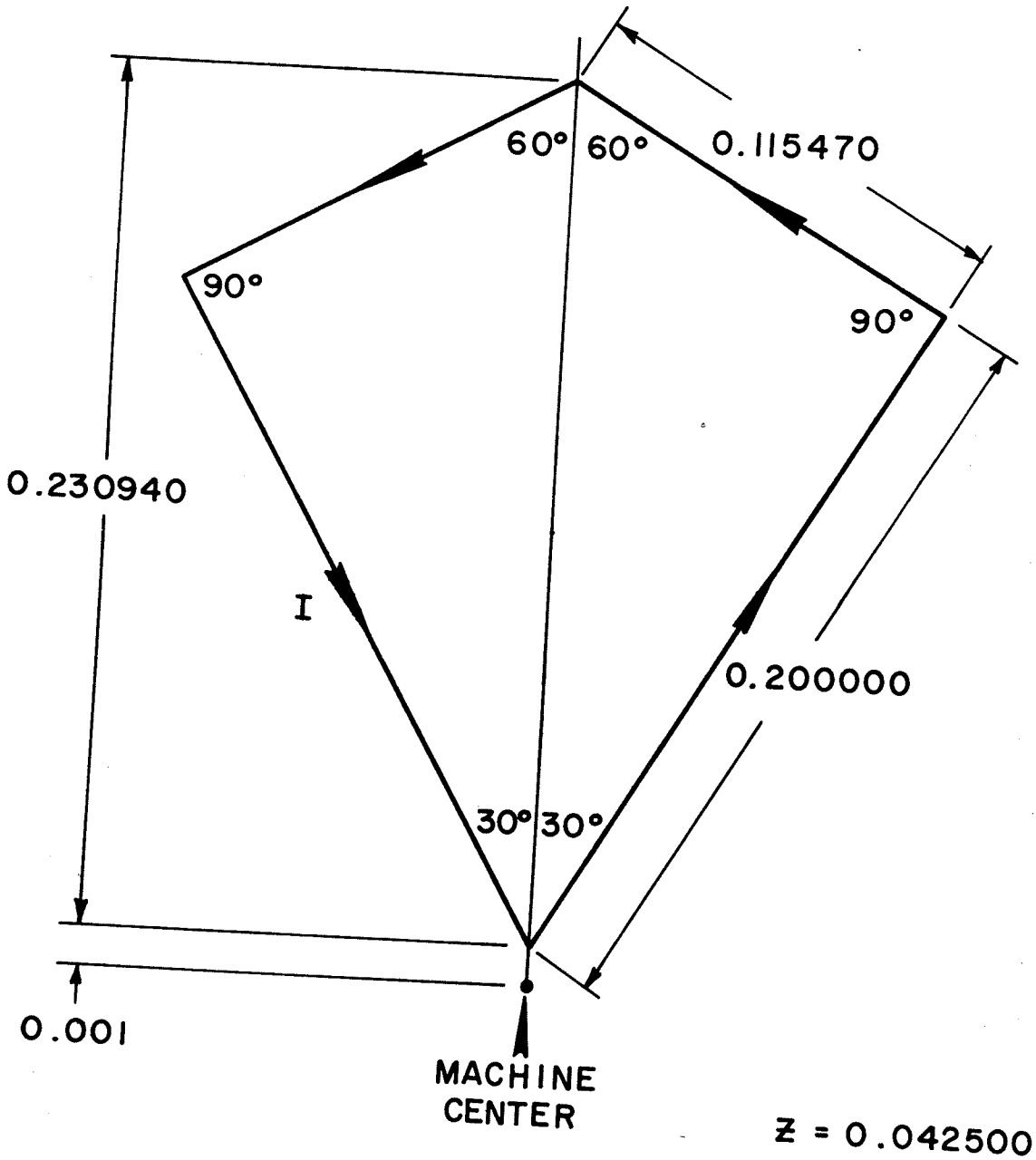

Fig. 2: Geometry of the flutter coils.

The shape of an equilibrium orbit in such a magnetic field is given to first order by the expression

$$r(\theta) = r_o \left(1 + \sum_n \frac{f_n(r)}{n^2-1} \cos n\theta \right)$$

when the field is expressed in the form

$$B(r,\theta) = B_o \left(1 + \sum_n f_n (r) \cos n\theta \right).$$

Because of the symmetries chosen, only the cosine components of order 3n appear in the expansion. The amplitude of each successive harmonic was found to be down by more than an order of magnitude from the preceding one. Since the effect of the $n^{\underline{th}}$ harmonic on the shape of the trajectory goes roughly as $\frac{f_n}{(n^2-1)}$, only the third harmonic was retained for use in the equilibrium orbit code. The sector coil flutter is then given by

$$F(r) = \frac{H_3^2 (r)}{2\overline{B}^2(r)}.$$

The sector coil current was adjusted such that this flutter matched as nearly as possible the ideal flutter. The resulting flutter is plotted in Figure 3 with the ideal flutter as a function of radius. With this flutter field, the isochronous average field and equilibrium orbits were calculated. The resulting isochronous average field is shown in Figure 4, and the equilibrium orbit properties

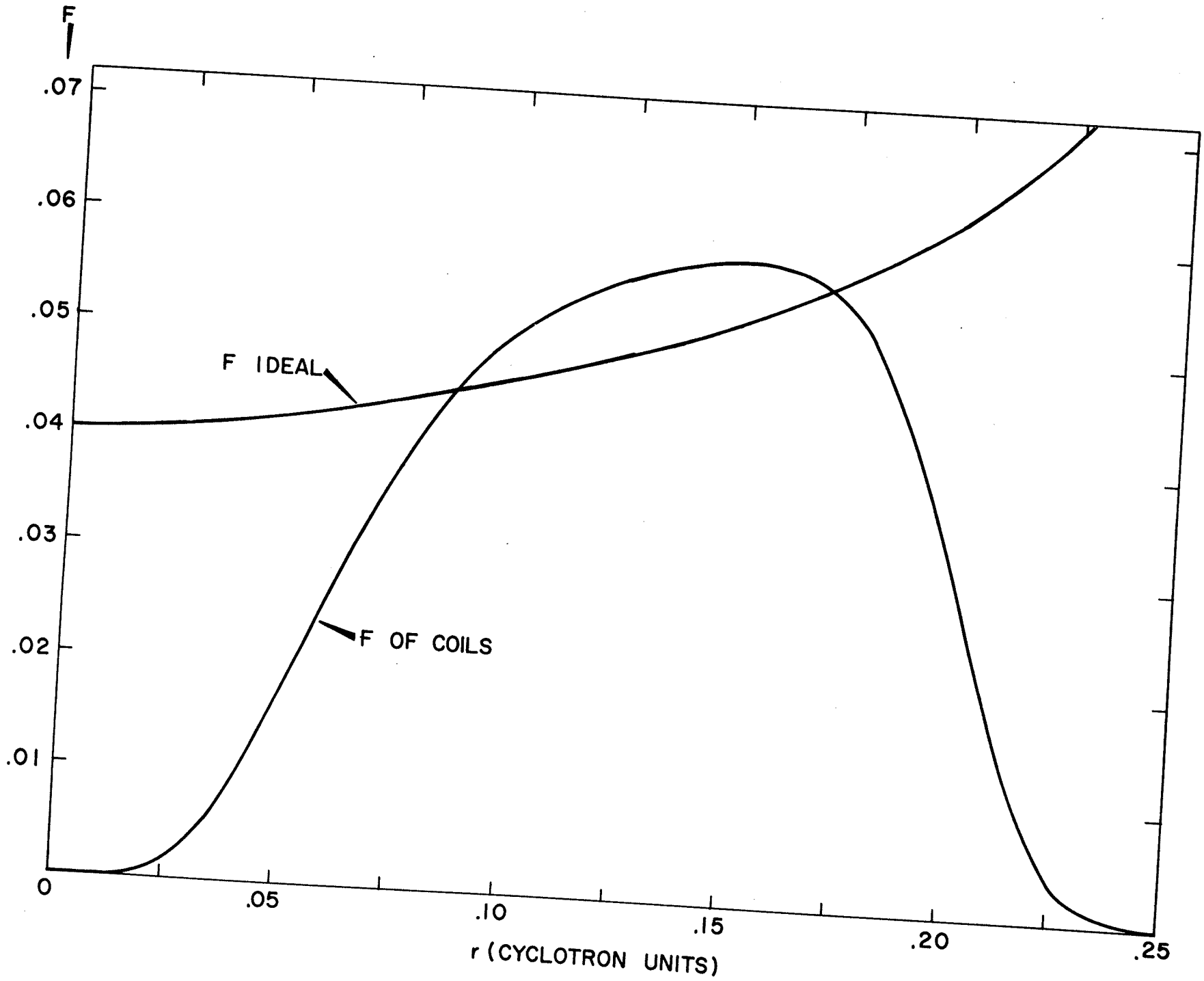

Fig. 3: Flutter produced by the system of six flutter coils.

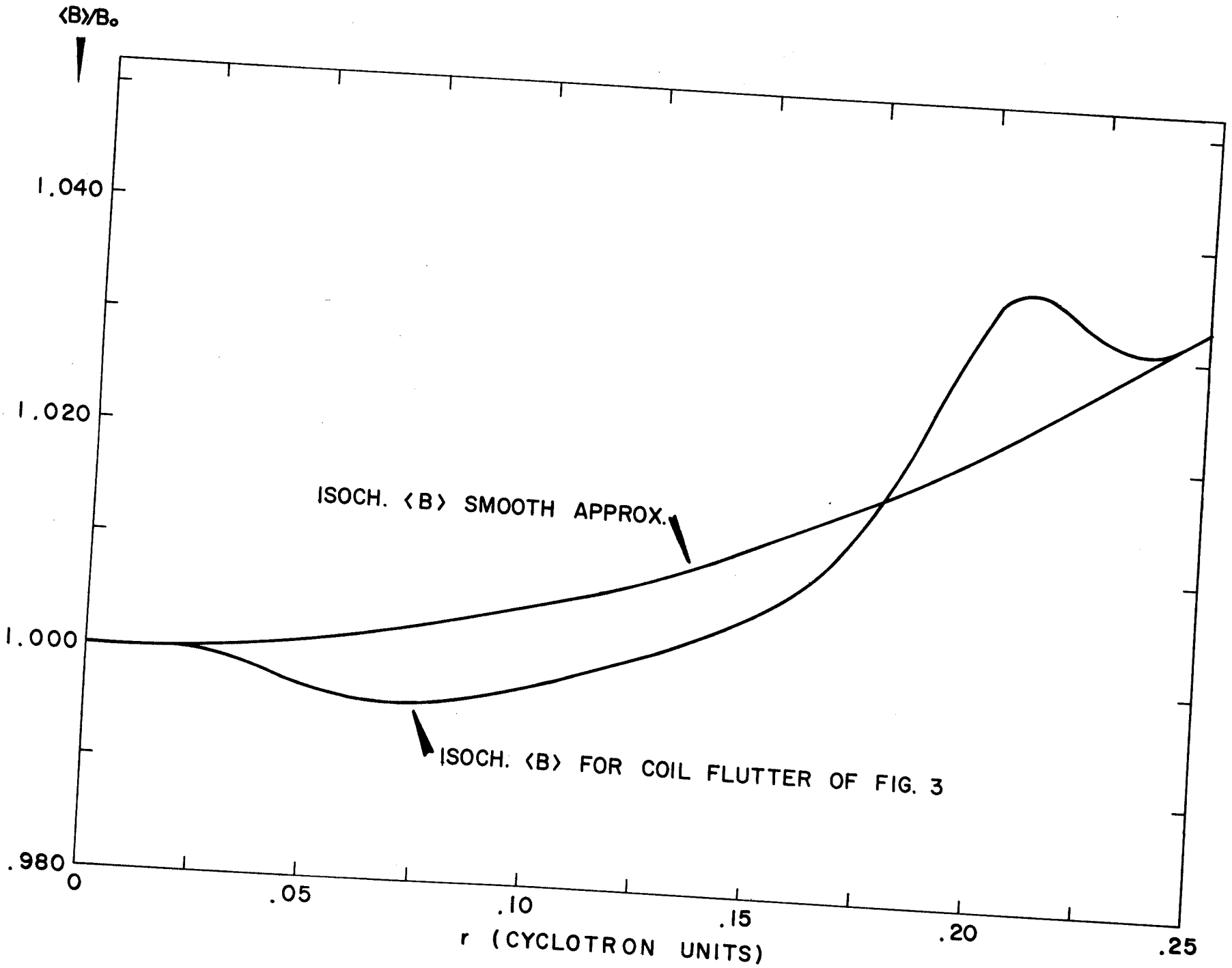

Fig. 4: Ideal isochronous average field for flutter of Figure 3.

summarized in Table 2, for the combination of the flutter coil and its ideal isochronous average field. The results indicate that such a flutter field produced by the chosen coil set is an acceptable choice.

The isochronous average field minus the average field of the flutter coils must be produced by a group of circular coils; this field is shown in Figure 5. The average field must be isochronous only to the extraction radius; beyond this it may fall with radius. This also, by equation (3), insures that the $\nu_r = 1$ resonance occurs at the extraction energy. Therefore, the ideal average field was matched out to this radius (40 Δr steps) and allowed to fall off normally after this point.

In order to avoid inefficient current arrangements (neighboring coils carrying large oppositely-directed currents) which often result from least square computations, the matching of the ideal field was accomplished in three steps. The shape of the ideal average field of the circular coils, shown in Figure 5, suggests that it may be matched most efficiently for a first approximation by two main coils. A pair of turns which matched this most closely with a least squares fit was found; the resulting matched field and residue are also shown in Figure 5. The resulting error with this fit is less than 5% of the original field.

Table 2. Equilibrium orbits in the field composed of the flutter field of Figure 3 and its ideal isochronous average field.

1000010000 +187549600 10 HEX RK STEPS +00500000 =R INC.

E	R AV	PHASE	R	PR	NU R	NU Z		
+000100	+032632	+000006	+033025	+000000	+100522	+010137	1N	01
+000200	+046098	+000001	+047091	-000000	+101287	+016142	1J	01
+000400	+065062	+000000	+067136	-000000	+102174	+020952	1N	01
+000600	+079562	-000000	+082494	-000000	+102550	+022539	1N	01
+000800	+091756	-000001	+095384	-000000	+102732	+023064	1L	01
+001200	+112149	-000000	+116866	-000000	+102937	+022978	1-	00
+001600	+129269	-000001	+134837	-000000	+103116	+022340	1N	00
+002000	+144286	-000004	+150563	-000000	+103275	+021375	1N	00
+002400	+157805	-000019	+164669	-000000	+103291	+019818	1N	00
+002800	+170195	-000064	+177469	-000000	+102959	+017149	1N	00
+003200	+181724	-000088	+189087	-000000	+102007	+016201	1N	00
+003600	+192615	+000061	+199533	-000000	+101164	+024936	1N	00
+003800	+197850	+000134	+204301	-000000	+101413	+031747	1J	00
+003900	+200411	+000143	+206574	-000000	+101700	+035209	1N	00
+004000	+202935	+000129	+208778	-000000	+102125	+038165	1-	00
+004200	+207874	+000071	+213008	-000000	+102974	+042950	1N	01

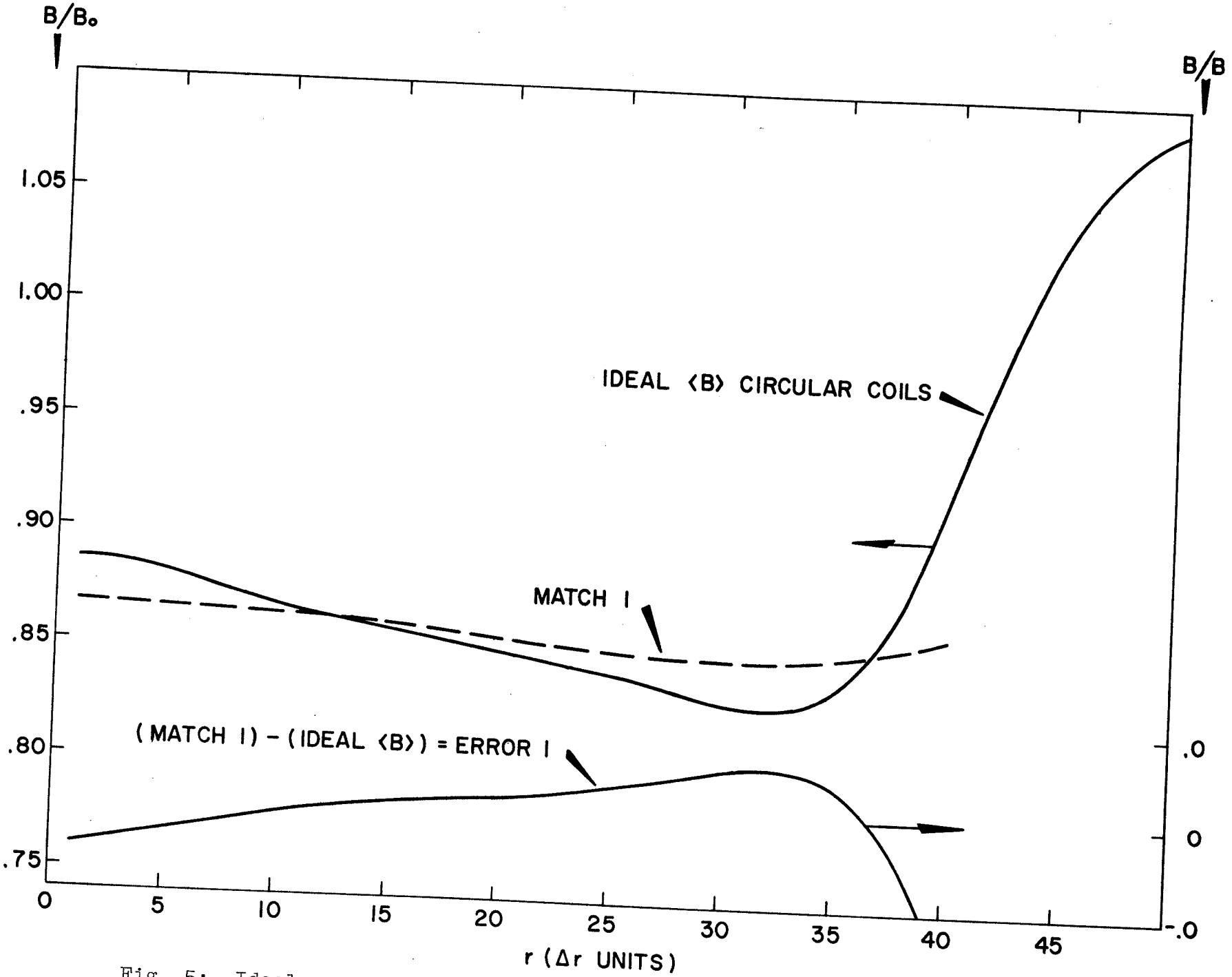

Fig. 5: Ideal average field of the circular coils (isochronous average field minus average field of flutter coils); match of this with two main coils, and residual field.

The shape of the residual field suggests that it may most readily be produced by a small turn near the center and a pair of larger coils, closely spaced with opposing currents. A triplet of coils which most nearly matched the desired curve was found, and the resulting fit and residue plotted in Figure 6. It was found that this fit reduces the error by approximately an order of magnitude, while requiring currents down more than an order of magnitude from the currents in the main coils.

The equilibrium orbits in the resulting field were found, and the $\nu_r = 1$ resonance observed to occur early, which would result in an energy loss in the extracted beam. Therefore, the field was altered slightly by increasing the current in one of the secondary coils to postpone the resonance until the desired extraction energy.

Equilibrium orbits were then found in the corrected field. The phase of an accelerating particle is given by[19]

$$\sin \Phi\ (E) = \sin \phi_o + \frac{2\pi}{V} \int_o^E \left(1 - \frac{\omega_{rf}}{\omega_o(E)} \right) dE$$

where in this case $\phi_o = 0^o$, V is the voltage gain per revolution, and ω_{rf} is the angular frequency of the r.f.

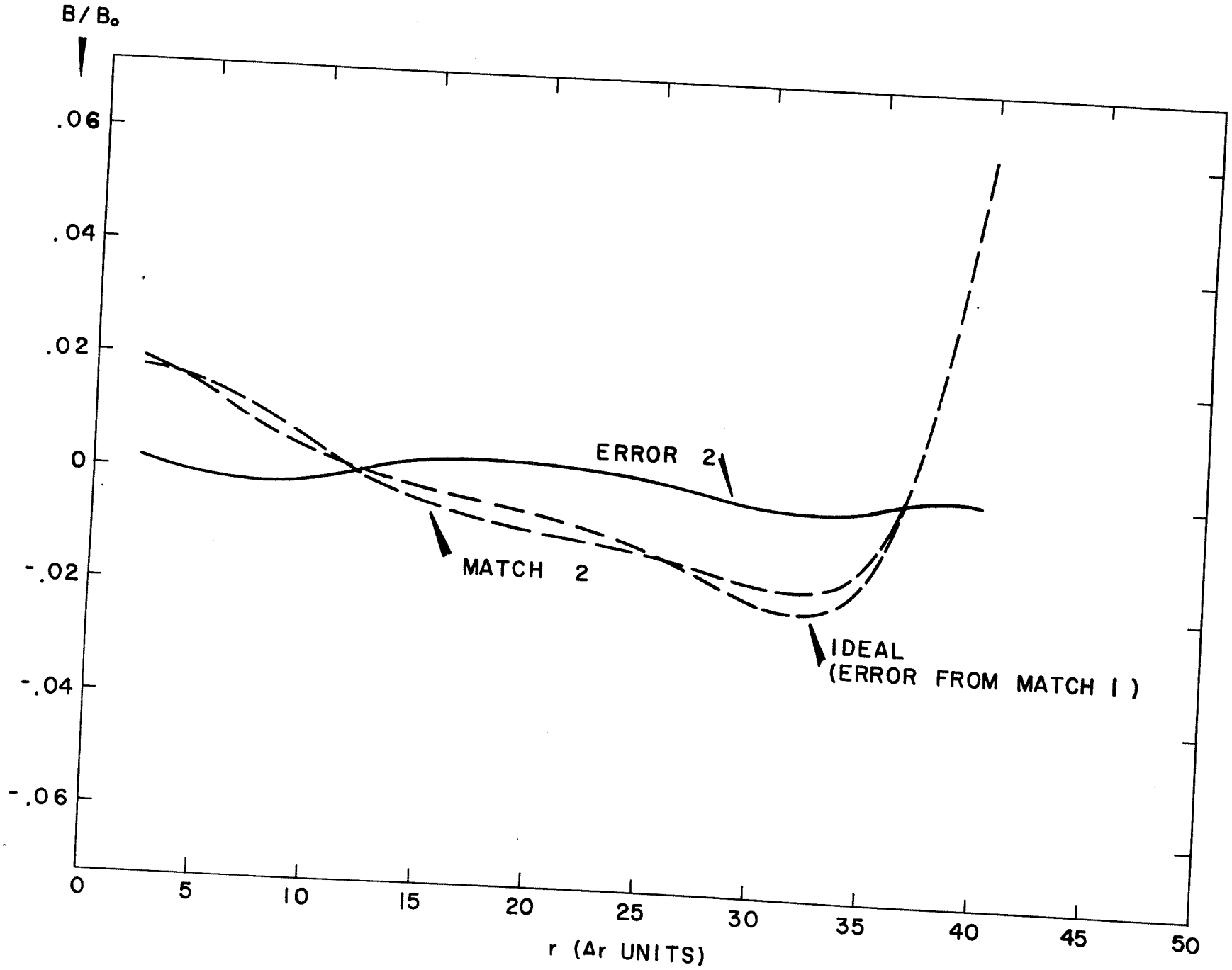

Fig. 6: Match of residual field (Figure 5) by secondary coils.

accelerating voltage. The results of this calculation are indicated in Figure 7 for a voltage gain per turn of 280 kilovolts. By scaling the field values and the cyclotron unit by a small amount, the phase can be minimized; here the phase at 40 Mev, the extraction energy, was set approximately equal to zero. The results of the scaling are also shown in Figure 7. This was found to be an acceptable basic field, the resonance appearing at the correct energy and the phase not becoming excessive as the particle accelerates up through the extraction energy.

Finally, this field was corrected to give the desired phase limits by a carefully selected set of trimming coils. The final error in the ideal-matched fields was less than 0.02%, and the currents in the trimming coils were found to be down approximately one order of magnitude from the currents in the secondary coils.

A set of equilibrium orbits was found in the final field, and is presented in Table 3. The field satisfies the extraction requirements, as well as the basic focusing and isochronism requirements to within the specified tolerances.

A summary of the coil data from the above field fittings is presented in Table 4, where the central magnetic field is approximately 14 kilogauss. Several observations may be made concerning these data. The procedure used has led to the

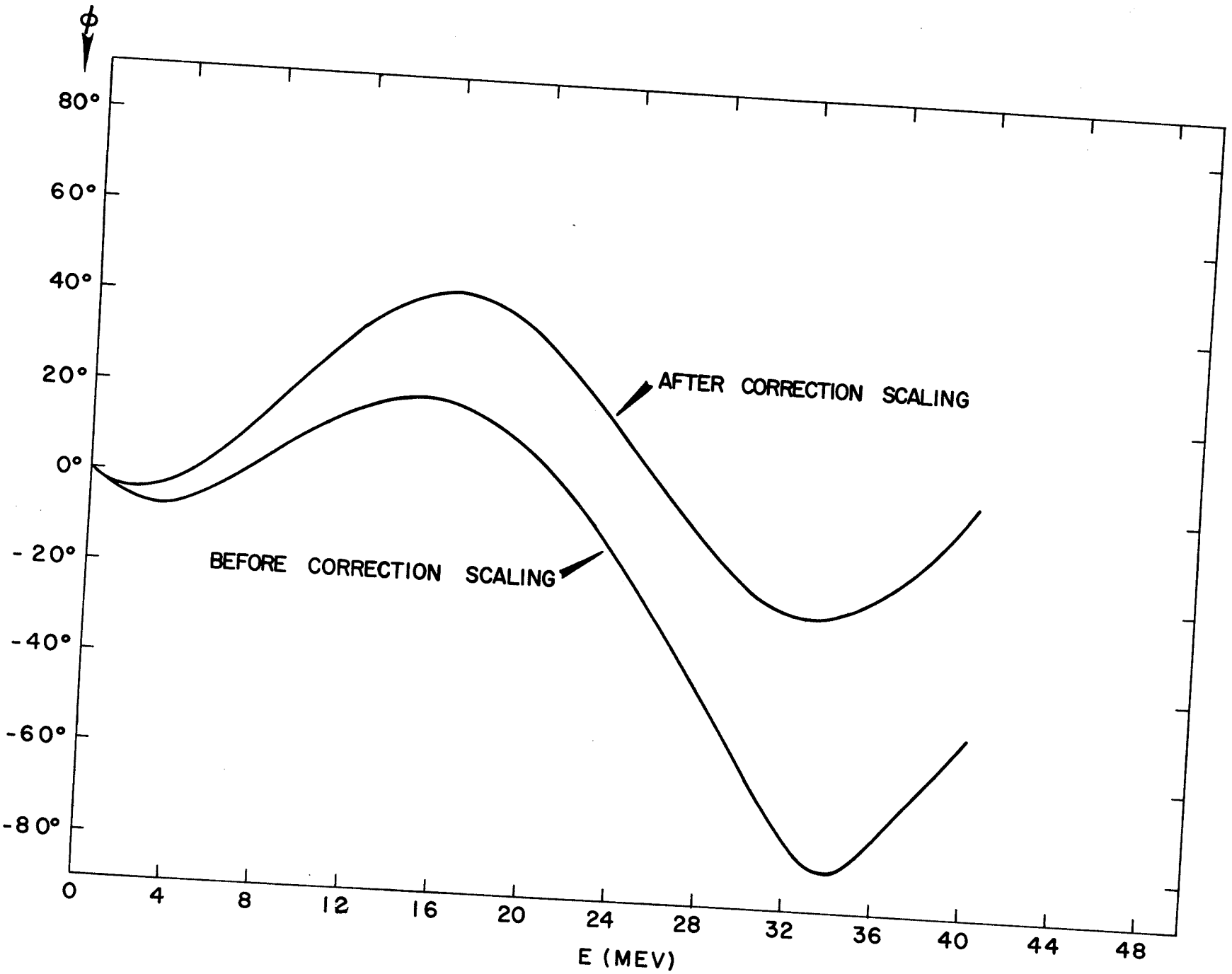

Fig. 7: Phase vs. energy before and after scaling trial field to minimize phase slip.

Table 3. Equilibrium orbits in the field produced by the flutter of Figure 3 and average field matched with the three sets of circular coils.

1000010000 +187549600 10 HEX RK STEPS +00500000 =R INC.

E	R AV	PHASE	R	PR	NU R	NU Z	
+000100	+032629	-000017	+033015	+000000	+100541	+009538	1N 01
+000200	+046075	-000091	+047047	+000000	+101316	+015299	1N 01
+000400	+065023	-000115	+067053	-000000	+102111	+020469	1J 01
+000600	+079503	-000143	+082372	-000000	+102411	+022170	1J 01
+000800	+091686	-000151	+095237	-000000	+102681	+022275	20 01
+001200	+112056	-000165	+116672	-000000	+102863	+022291	1J 01
+001600	+129172	-000153	+134620	-000000	+102944	+022074	1N 00
+002000	+144203	-000124	+150348	-000000	+103132	+021022	1N 00
+002400	+157707	-000134	+164429	-000000	+103390	+018754	1N 00
+002800	+170111	-000120	+177228	-000000	+102931	+018794	1N 00
+003200	+181790	+000020	+188993	-000000	+102392	+020704	1N 00
+003600	+192855	+000195	+199617	-000000	+101702	+028337	1L 01
+003800	+198245	+000554	+204512	-000000	+100906	+039374	1- 00
+003900	+200956	+000901	+206897	-000000	+099942	+046484	1J 01
+004000	+203722	+001275	+209287	-000000	+098298	+053869	1N 01
+004200	+209668	+002811	+214325	-000000	+092020	+069244	1N 01

Table 4. Relative currents in the several coils used to produce the field (E0's in Table 3).

Coil Sectors		Relative Currents
Main Coils	#1	0.0226
	#2	1.0000
		0.3071
Sec. Coils	#1	
	#2	0.0324
	#3	-0.0257
		0.0074
Trim. Coils	#1	
	#2	0.0100
	#3	+0.0004
	#4	0.0002
	#5	0.0044
		-0.0069

1 unit ~ 6.5×10^6 ampere turns.

satisfactory condition of having most of the average field produced by two main coils, the rest being produced by two groups of smaller coils, whose ampere-turn requirement is down considerably from the main coils. The spacing of the coils (discussed in detail in a following section) will not interfere with other necessary parts of the machine, such as dees, which must be placed inside the lowest coil layer. Further, most of the coils are located in a relatively small volume, which simplifies the necessary cooling apparatus.

Having developed a set of coils which will adequately produce the fields for the preliminary run, it is necessary to make a somewhat arbitrary choice of cyclotron parameters. Desiring the cyclotron to yield 40 Mev protons, the hydrogen cyclotron unit was chosen as 2.25 meters (approximately 88.5 inches). This fixed the central field at 13.93 kilogauss. The spacing between the radii where fields were stored was then 0.615 inches. These choices give the following extraction energies for the respective particles: 40 Mev protons, 20 Mev deuterons, 50 Mev C^{4+} ions, keeping the central field and the radial spacing constant.

Using the chosen coils, a procedure similar to that indicated above was then used to obtain empirical fields for the three particles at the above energies. The resulting average field and third harmonic are shown for H^+, D^+, and

C^{4+} ions in Figures 8, 9, and 10 respectively. Tables 5, 6, and 7 indicate the properties of the equilibrium orbits in the three respective cases. Figures 11-16 show the axial and radial focusing frequencies, and the phase as a function of energy. Table 8 presents programs for the coils to produce each of the three fields. The radius and distance from the median plane of each coil is given, along with its respective current. The cross-sectional area necessary for each of these wire bundles was then calculated, using an accepted value[20] of the allowable current density with a 25% safety factor, and is shown in Table 9. One-quarter of the cross-sectional view of the final superconducting coil arrangement is shown in Figure 17. The space occupied by the sector coils (Figure 2) is indicated by the slanted lines. For the purpose of the field matching, several of the individual turns have been used more than once, the total current being indicated in the table. This set of superconducting elements is then sufficient to produce isochronous cyclotron fields for 40 Mev H^+, 20 Mev D^+, and 50 Mev C^{4+} ions.

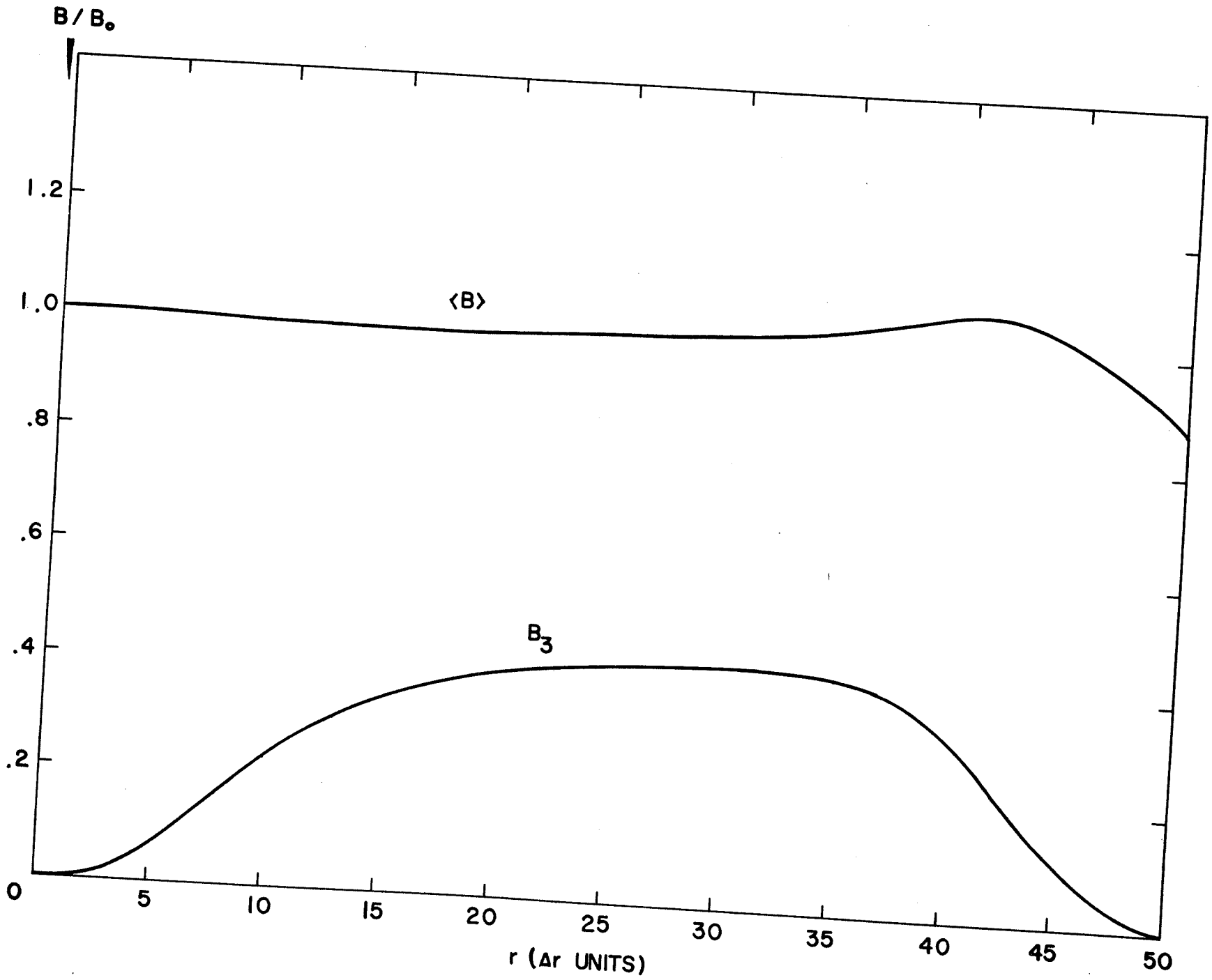

Fig. 8: <B> and B_3 for the 40 Mev H^+ field.

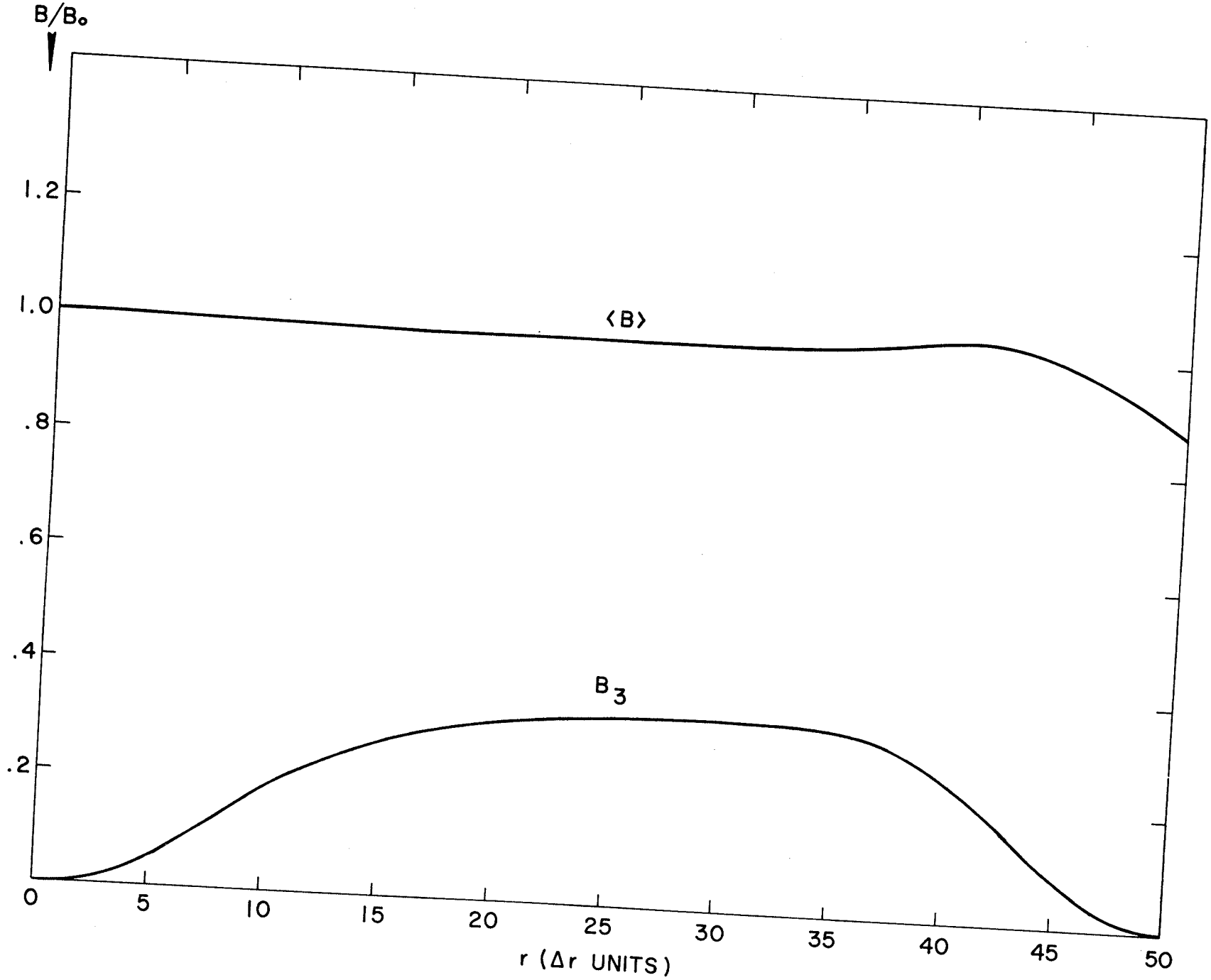

Fig. 9: ⟨B⟩ and B_3 for the 20 Mev D^+ field.

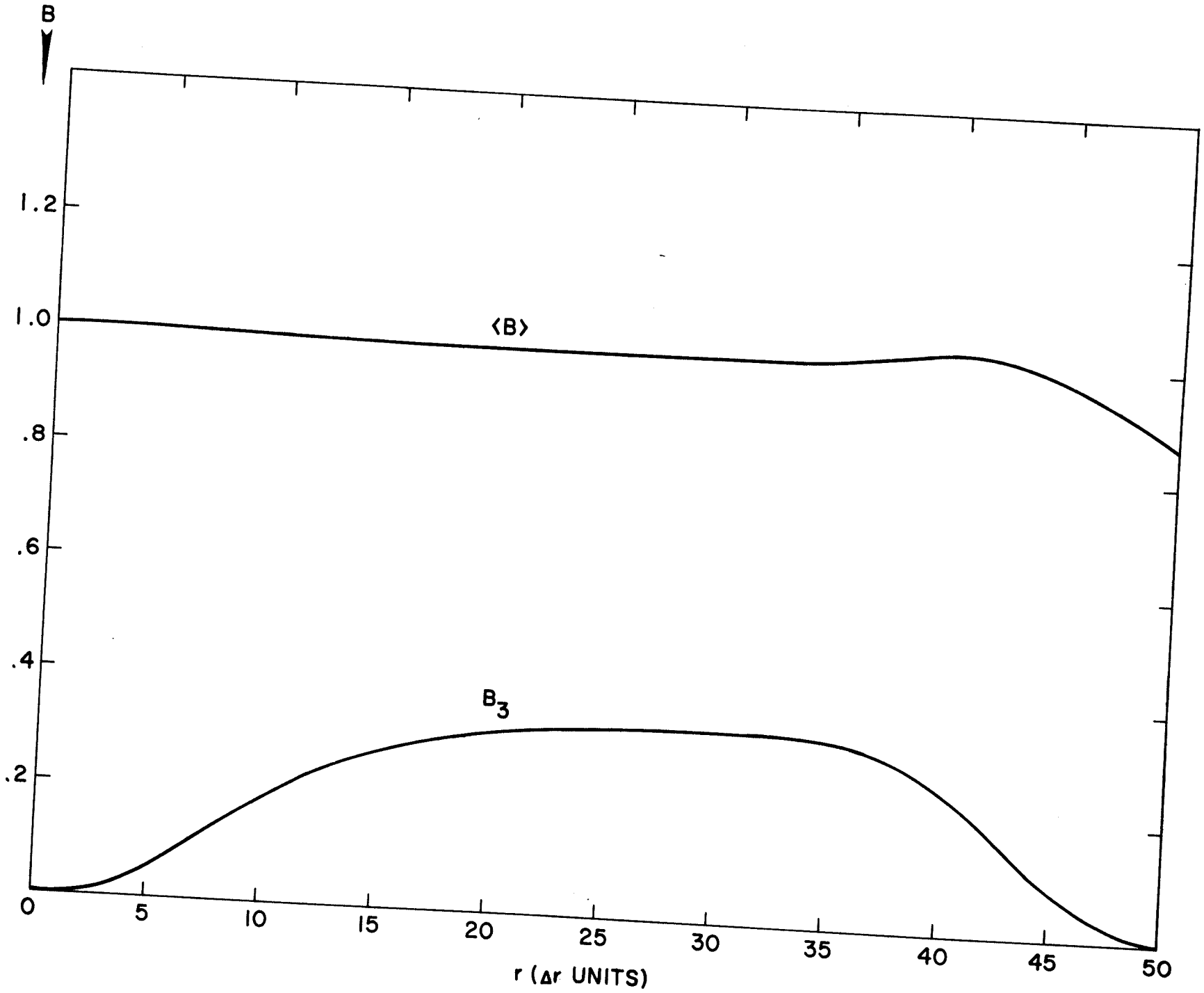

Fig. 10: ⟨B⟩ and B_3 for the 50 Mev C^{4+} field.

Table 5. Equilibrium orbits in the 40 Mev H^+ field.

1000010000 +938230000 10 HEX RK STEPS +00695423 =R INC.

E	R AV	PHASE	R	PR	NU R	NU Z	
+001000	+046115	+000123	+046818	-000000	+100886	+012275	1N 01
+002000	+065071	-000240	+066826	-000000	+102090	+019626	1J 01
+004000	+091738	+000051	+095367	-000000	+103344	+025809	1N 01
+006000	+112086	+000337	+117193	-000000	+104028	+027239	1N 01
+008000	+129136	+000323	+135430	-000000	+104430	+027330	1N 01
+012000	+157517	+000039	+165647	-000000	+104855	+026579	1L 01
+016000	+181282	+000105	+190835	-000000	+105031	+025952	1N 00
+020000	+202076	+000351	+212812	-000000	+105496	+023851	1N 00
+024000	+220616	+000071	+232317	-000000	+105974	+019322	1N 00
+028000	+237527	-000270	+249859	-000000	+105038	+016620	1N 00
+032000	+253361	+000002	+265782	-000000	+103554	+015872	1J 01
+036000	+268312	+000431	+279929	-000000	+102274	+029715	1- 00
+038000	+275589	+000933	+286331	-000000	+101792	+044312	1J 01
+039000	+279241	+001455	+289417	-000000	+101111	+052747	1- 01
+040000	+282954	+002338	+292483	-000000	+099876	+061494	1- 01
+042000	+290963	+006526	+298935	-000000	+092781	+079762	1J 01

Table 6. Equilibrium orbits in the 20 Mev D^+ field.

1000020000 +187549600 10 HEX RK STEPS +00347890 =R INC.

E	R AV	PHASE	R	PR	NU R	NU Z	
+000100	+032606	-000098	+033312	-000000	+101270	+016242	1J 01
+000200	+046044	+000035	+047509	-000000	+101960	+021603	1N 01
+000300	+056342	+000251	+058406	-000000	+102290	+023166	1J 01
+000400	+065007	+000290	+067557	-000000	+102457	+023637	1J 01
+000600	+079505	+000099	+082813	-000000	+102588	+023775	1N 01
+000800	+091718	+000130	+095623	-000000	+102511	+024211	1N 01
+001000	+102470	+000286	+106875	-000000	+102649	+023408	1N 01
+001200	+112133	+000025	+116943	-000000	+102722	+021216	1J 00
+001400	+121028	-000117	+126078	-000000	+101644	+021362	1F 01
+001600	+129384	+000172	+134389	-000000	+100652	+022397	1J 01
+001700	+133371	+000202	+138186	-000000	+100339	+026965	1N 01
+001800	+137281	+000405	+141760	-000000	+099515	+037994	1J 01
+001900	+141243	+001632	+145227	-000000	+096950	+053419	1J 01
+002000	+145553	+005830	+148875	-000000	+090166	+070289	1N 01

Table 7. Equilibrium orbits in the 50 Mev C^{4+} field.

1000030000 +111754800 10 HEX RK STEPS +00233535 =R INC.

E	R AV	PHASE	R	PR	NU R	NU Z	
+000010	+013376	+000104	+013497	+000000	+100296	+008268	1N 01
+000020	+018903	-000027	+019232	+000000	+100891	+013928	1N 01
+000030	+023135	-000156	+023675	-000000	+101341	+017539	1N 01
+000060	+032680	+000126	+033768	-000000	+102001	+022442	1F 01
+000090	+039996	+000286	+041506	-000000	+102266	+023829	1N 00
+000120	+046154	+000255	+048004	-000000	+102371	+024307	1N 00
+000180	+056472	+000056	+058851	-000000	+102354	+024832	1J 00
+000240	+065185	+000234	+067982	-000000	+102280	+025176	1N 00
+000300	+072842	+000172	+075983	-000000	+102449	+023576	1J 00
+000360	+079747	-000153	+083120	-000000	+101926	+023067	1N 00
+000420	+086170	+000153	+089561	-000000	+101431	+024079	1N 00
+000450	+089220	+000204	+092485	-000000	+101165	+028190	1N 00
+000480	+092201	+000425	+095215	-000000	+100186	+039882	1- 00
+000490	+093198	+000711	+096097	-000000	+099584	+045437	1J 01
+000510	+095241	+002065	+097864	-000000	+097067	+057436	1L 01

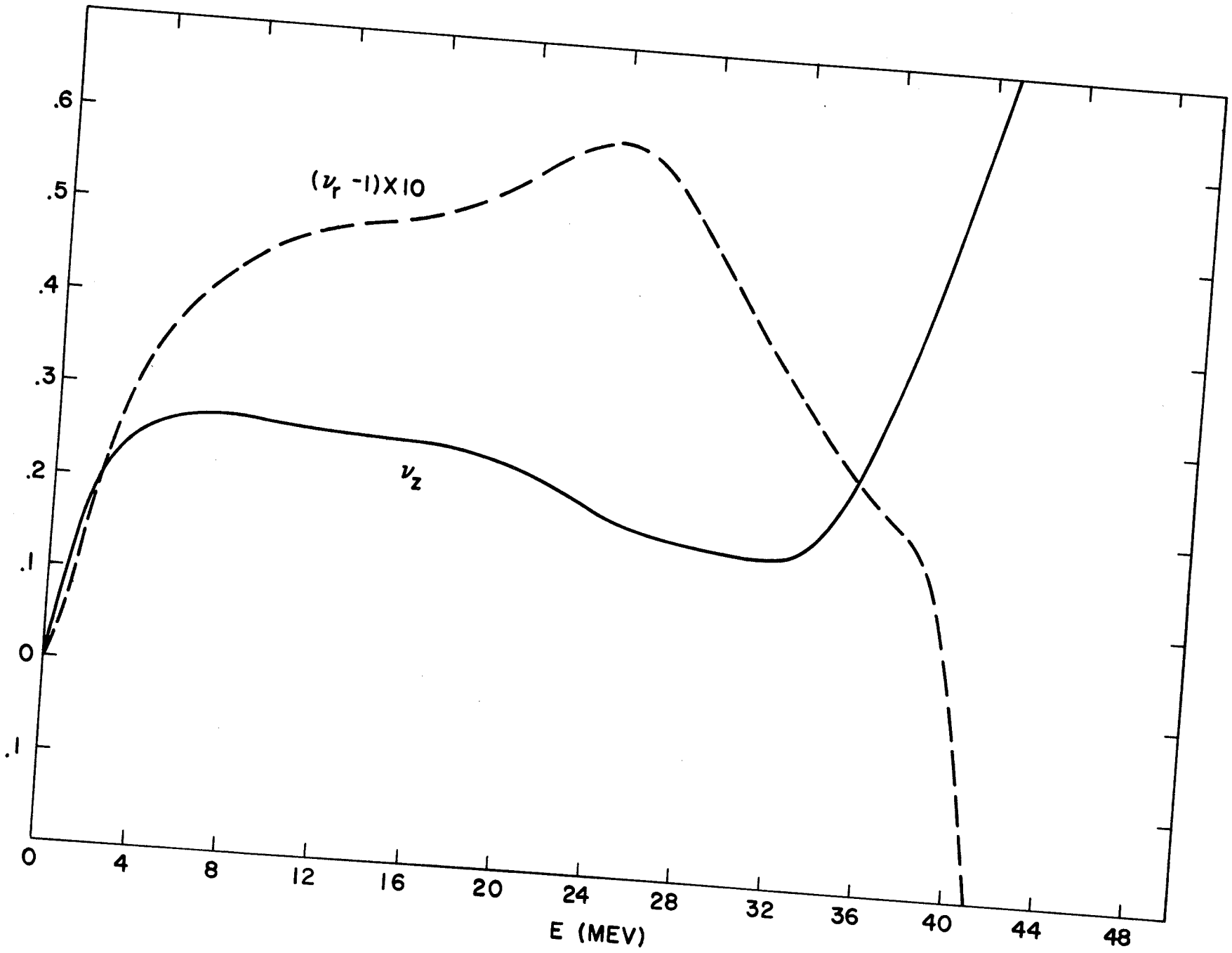

Fig. 11: ν_r and ν_z vs. energy for the H^+ field.

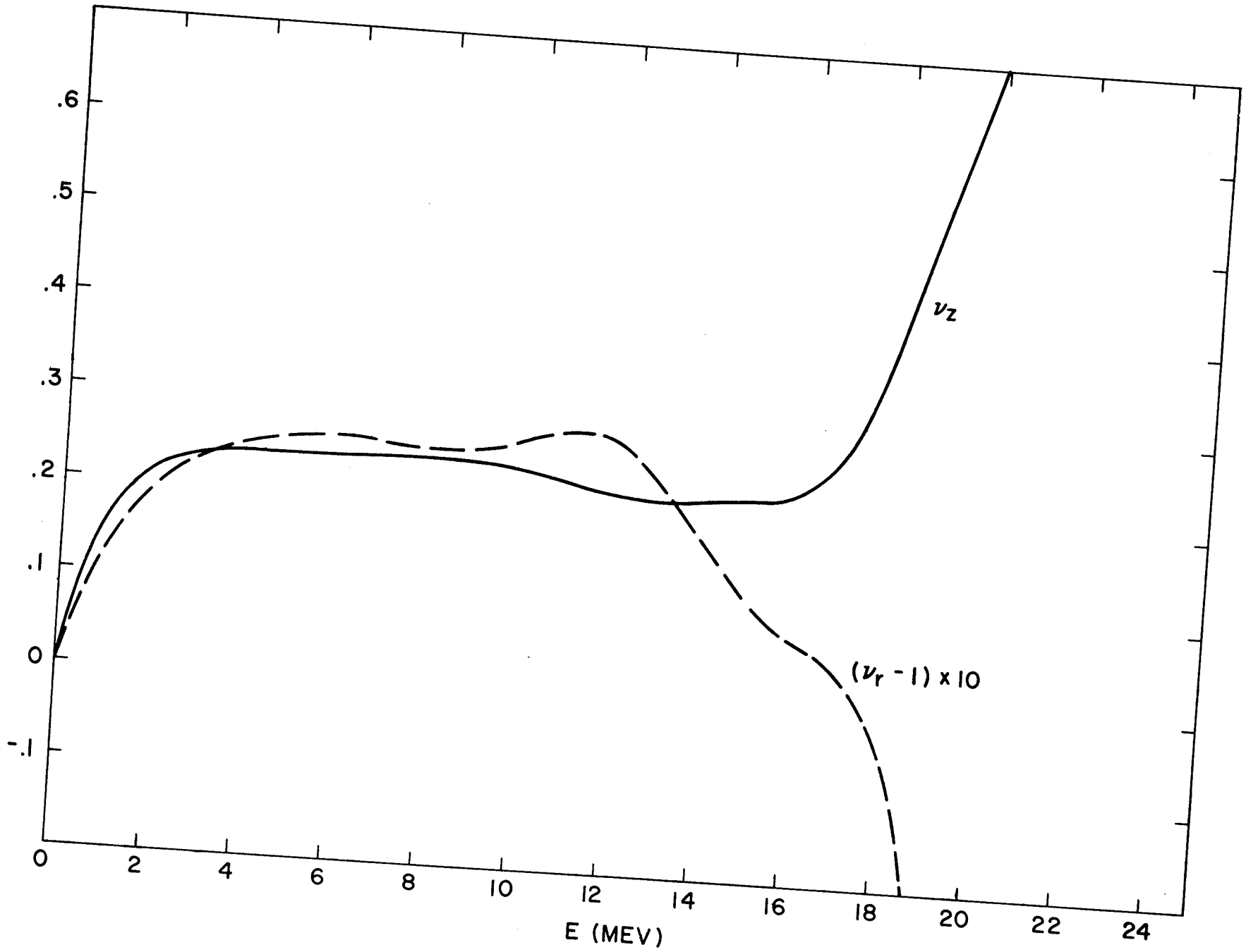

Fig. 12: ν_r and ν_z vs. energy for the D^+ field.

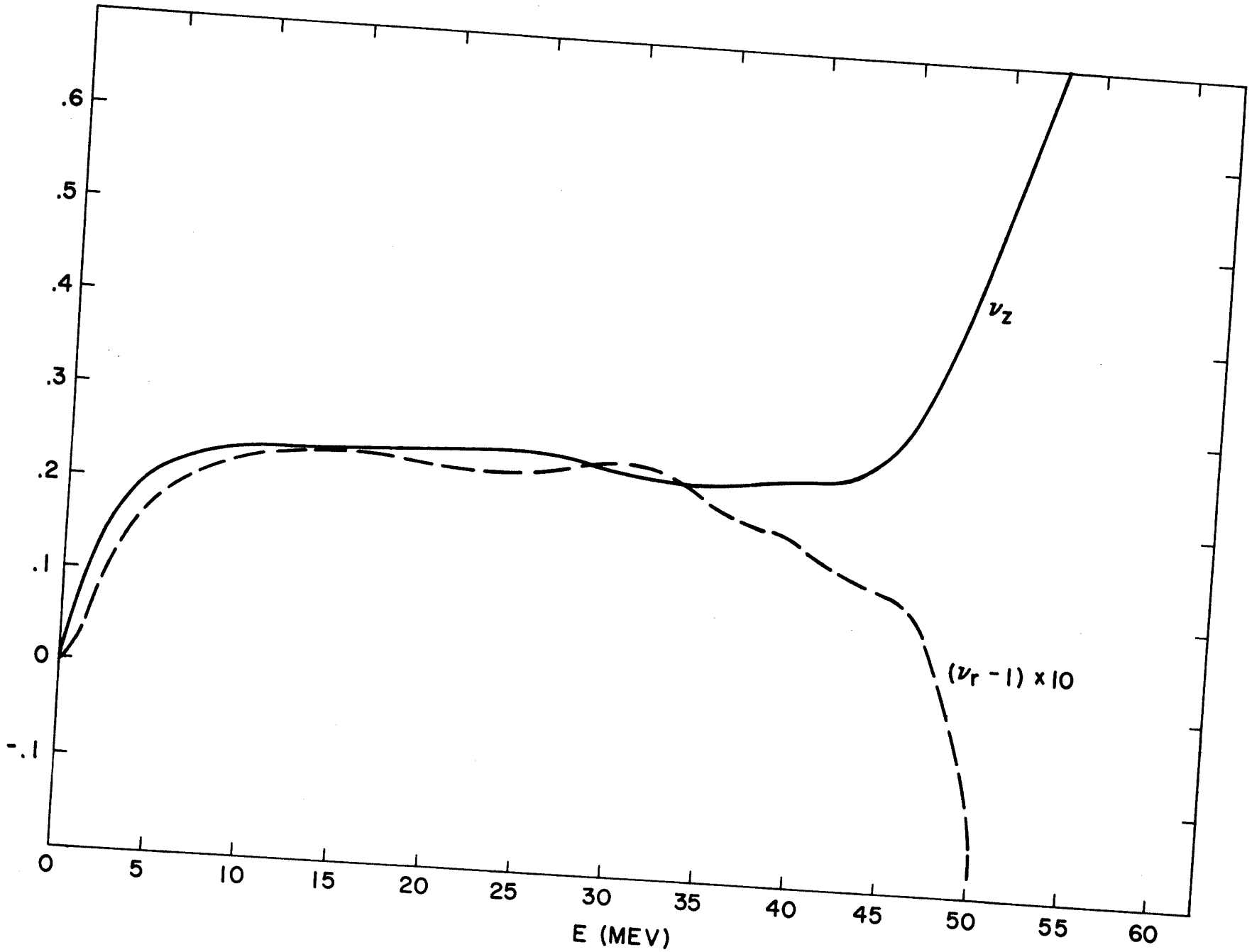

Fig. 13: ν_r and ν_z vs. energy for the C^{4+} field.

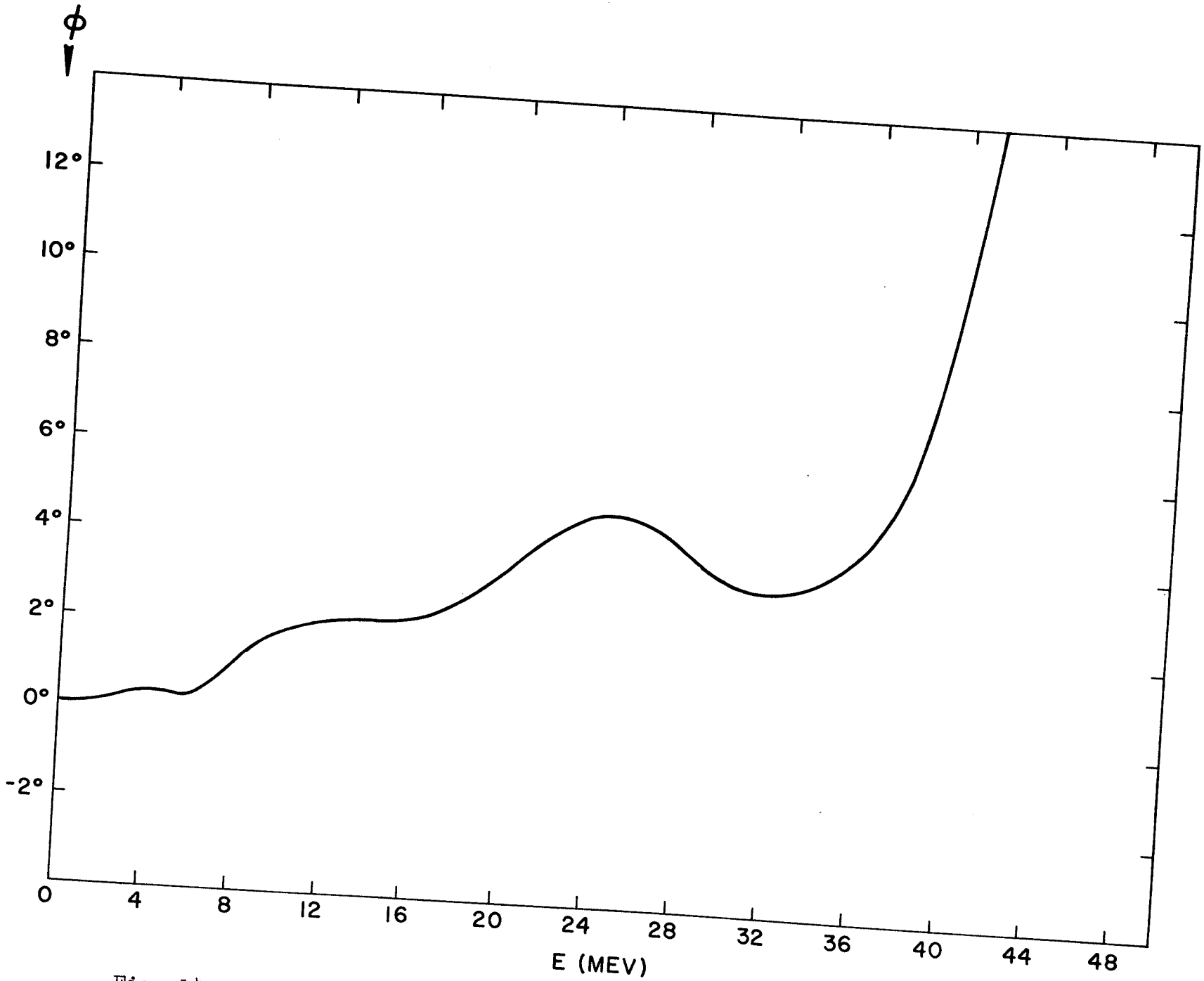

Fig. 14: Phase vs. energy for the H^+ field; first harmonic acceleration at 280 Kev per revolution maximum energy gain.

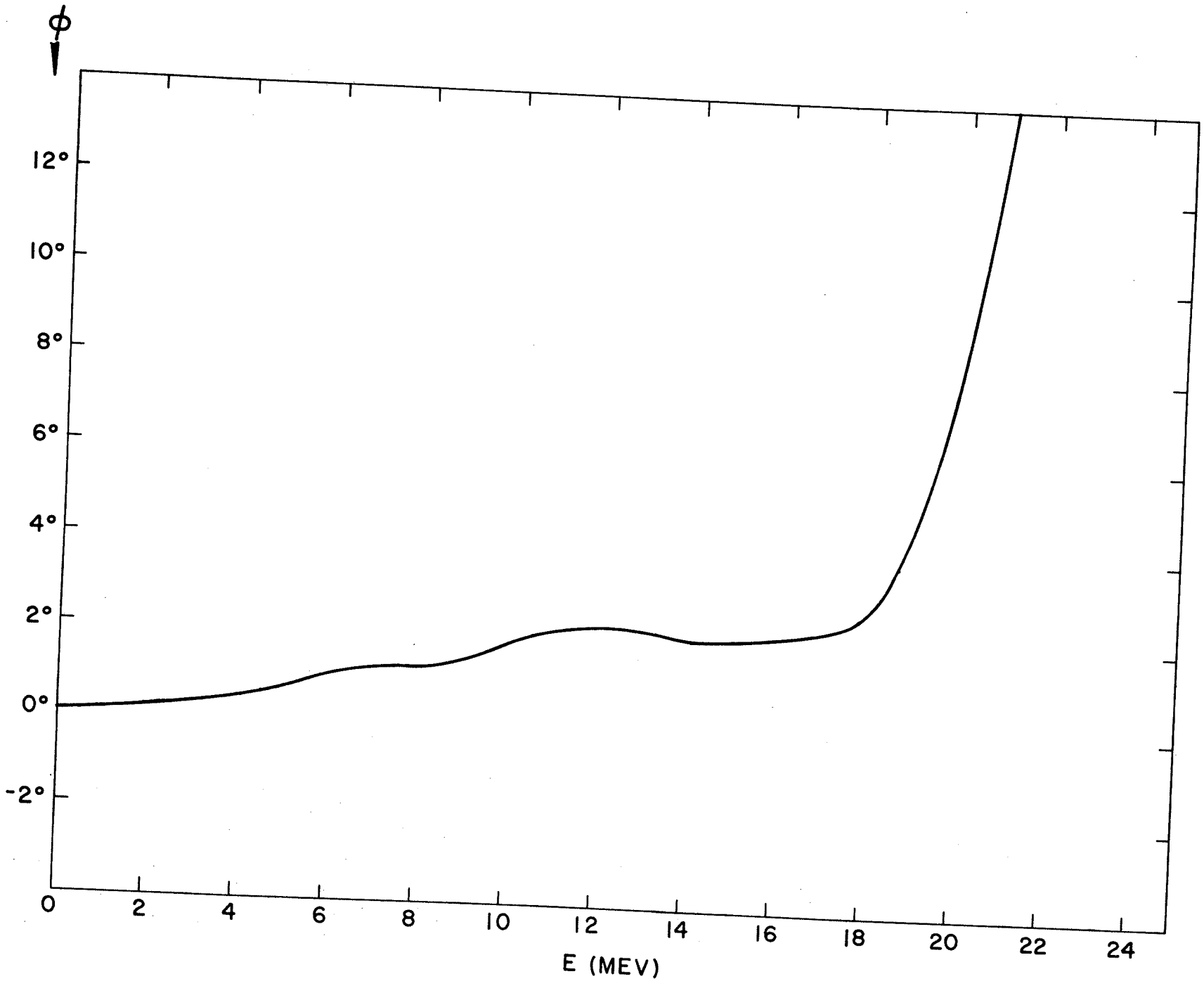

Fig. 15: Phase vs. energy for the D^+ field; first harmonic acceleration at 280 Kev per revolution maximum energy gain.

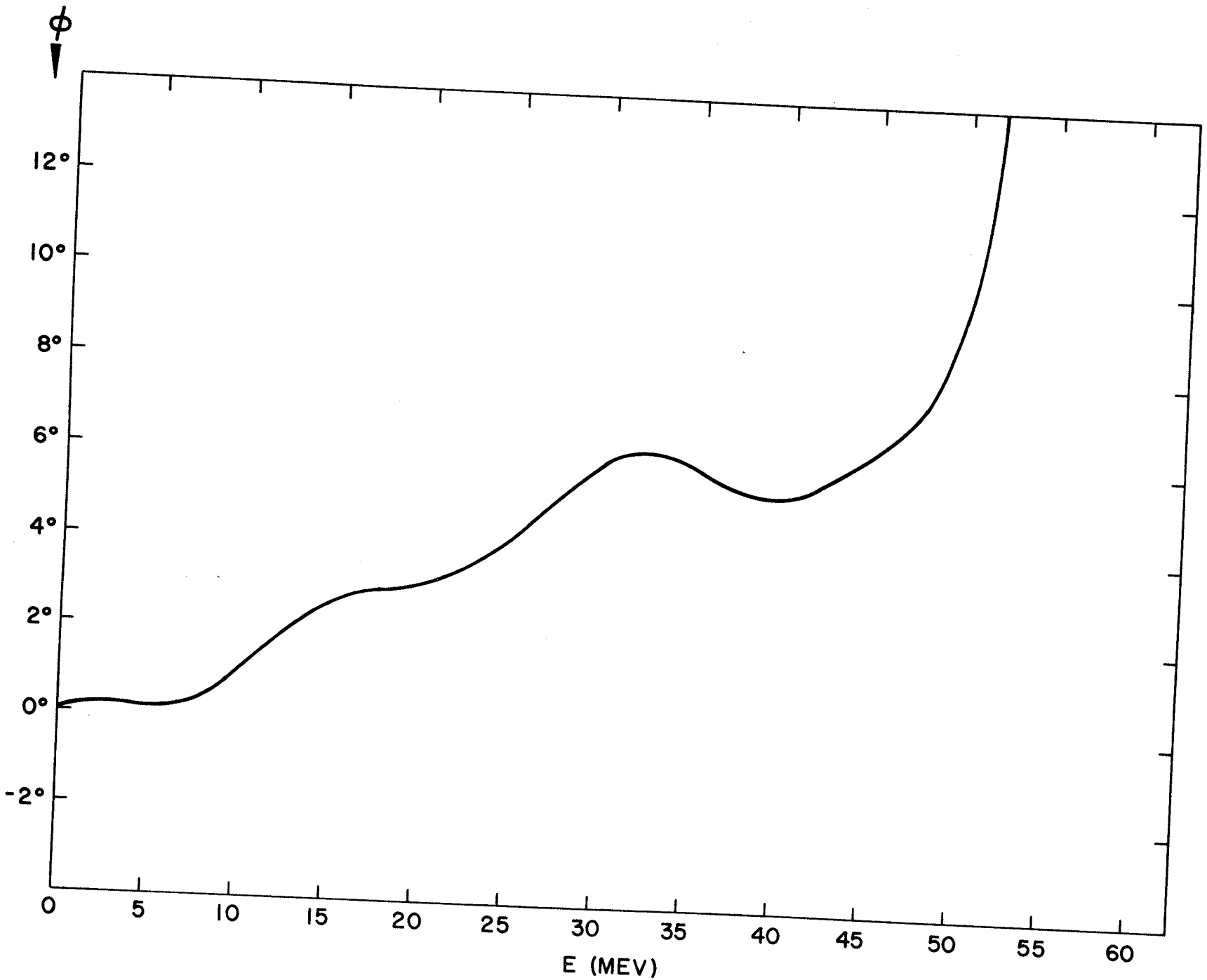

Fig. 16: Phase vs. energy for the C^{4+} field; first harmonic acceleration at 280 Kev per revolution maximum energy gain.

Table 8. Currents in the several coils used to produce the H^+, D^+, C^{4+} fields.

Coil	r(m.)	z(m.)	H^+	D^+	C^{4+}
Sector	~	.133	1.81×10^5	1.45×10^5	1.45×10^5
Main #1	.813	.813	5.78×10^6	6.43×10^6	6.52×10^6
#2	.923	.125	1.96×10^6	1.87×10^6	1.83×10^6
Sec. #1	.782	.094	2.22×10^5	1.83×10^5	1.83×10^5
#2	.626	.094	-1.56×10^5	-1.40×10^5	-1.39×10^5
#3	.157	.094	2.99×10^4	1.78×10^4	1.86×10^4
Trim. #1	.063	.094	7.71×10^4	6.30×10^4	6.23×10^4
#2	.220	.094	6.01×10^3	3.97×10^3	3.68×10^3
#3	.377	.094	3.60×10^3	1.79×10^3	2.06×10^3
#4	.471	.094	3.67×10^4	2.78×10^4	2.75×10^4
#5	.565	.094	-7.46×10^4	-4.50×10^4	-4.55×10^4

Table 9. Diameters of the coil windings necessary to carry the needed currents.

Coil		Diameter (inches)
Sector		1.30
Main	#1	7.50
	#2	4.20
Sec.	#1	1.60
	#2	1.51
	#3	0.77
Trim.	#1	0.82
	#2	0.23
	#3	0.18
	#4	0.57
	#5	0.81

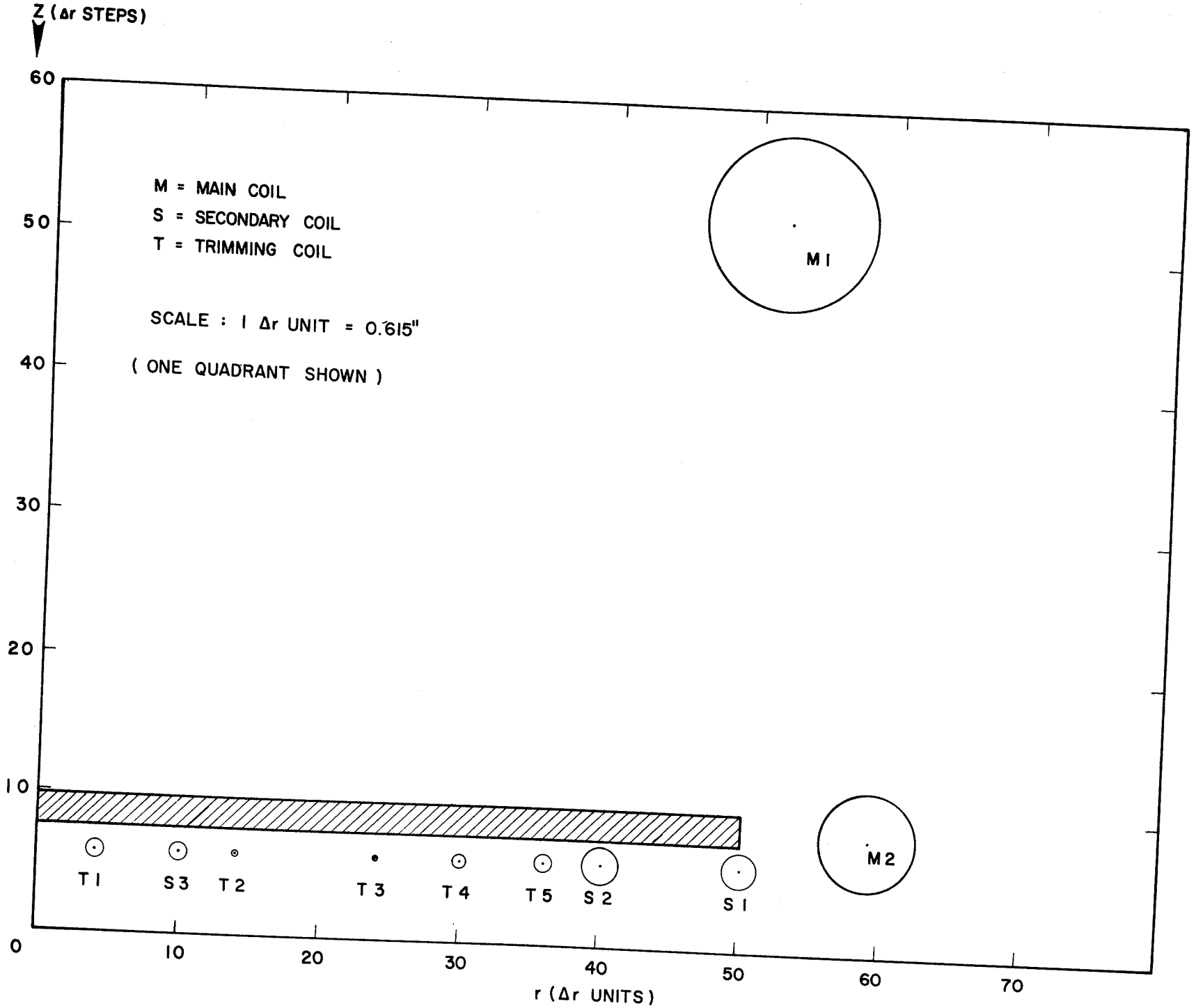

Fig. 17: Cross sectional view of final coil windings.

THE SUPERCONDUCTING MAGNET

To develop an initial acquaintance with the technological problems involved in a cyclotron of the sort here contemplated, a small solenoid was constructed using .040 inch Niobium-25% Zirconium wire.[21] The axial magnetic field at the center point of a thick solenoid (geometry shown in Figure 18), assuming a uniform current density is given by

$$B_z = \mu_o J l \log_\epsilon \left(\frac{b + \sqrt{l^2 + b^2}}{a + \sqrt{l^2 + a^2}} \right)$$

where J is the current density, l is the half-length of the solenoid, and a and b are respectively the inner and outer radii.

In view of the cost of the wire, the criterion ofr choosing the shape of the coil was minimization of the volume of the actual coil windings, or equivalently, minimization of the length of wire used to produce the desired field.[22] Having chosen the inner radius to leave enough space for a small search coil with which the field was measured, a short computer routine calculated the length and outer radius of the coil corresponding to the minimum volume of superconductor

necessary to produce a specified maximum field at the center of the coil. The coil specifications chosen were inner radius one centimeter, outer radius 2.3 centimeters, and length 2.8 centimeters.

The wire was insulated by a nylon serving and fusing process[23] which added approximately 0.002 inch to the outer diameter. The resulting coil, approximately 310 turns and requiring about 110 feet of insulated wire, was wound on a maple wood spool and potted in an epoxy resin.[24] The inductance of the coil was approximately 600 microhenrys, and its normal resistance approximately 15 ohms.

Two trials were made, the details concerning the experimental arrangement being somewhat different for each case. In both cases heavy copper wires were used for leads from the top of the Dewar to the coil. To minimize conduction of heat to the helium bath, the tops of these leads were kept in a liquid air bath. For the first trial, the current was taken from a 6-volt storage battery, and varied by means of a slide wire using .03 ohm per foot nichrome ribbon. The copper leads were mechanically clamped to the Nb-Zr coil leads. Due to the extremely sensitive adjustment necessary to increase the current to its maximum, this arrangement proved to be insufficient, so for the second trial the

current was obtained from a generator-regulator, in which the current adjustment was made with a potentiometer. In the second run the copper-Nb-Zr connection was also changed to a soldered joint. Since one cannot solder directly to Nb-Zr, the wire was first etched in a solution of hydrofluoric and nitric acids, then copper plated by electrolysis.[25] The copper plated Nb-Zr leads were soldered directly to the copper leads.

The basic circuit for the second trial is shown in Figure 19. To protect the coil from the surge voltage produced by the regulator when the coil went normal, a shunt of resistance approximately 0.1 ohm was provided. The shunt also provided a situation whereby the magnetic energy stored in the coil could be dissipated outside of the Dewar whenever the current was stopped. The safety precautions embodied in the shunt were found necessary to minimize the release of power to the helium bath and thus preserve the helium, and to prevent permanent changes in the properties of the superconducting wire which occur when large amounts of energy are dissipated therein.[26] Two methods were used to measure the field inside the superconducting coil. A small search coil consisting of 50 turns of number 38 enameled copper wire was wound on a half-inch wooden dowel and inserted into the center of the coil. A ballistic galvenometer was

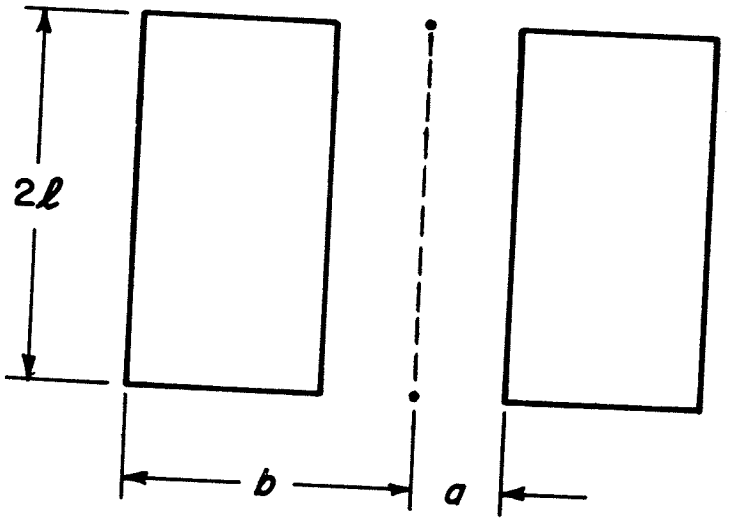

Fig. 18: Geometry of superconducting coil: a = 1 cm, b = 2.3 cm, 2ℓ = 2.8 cm.

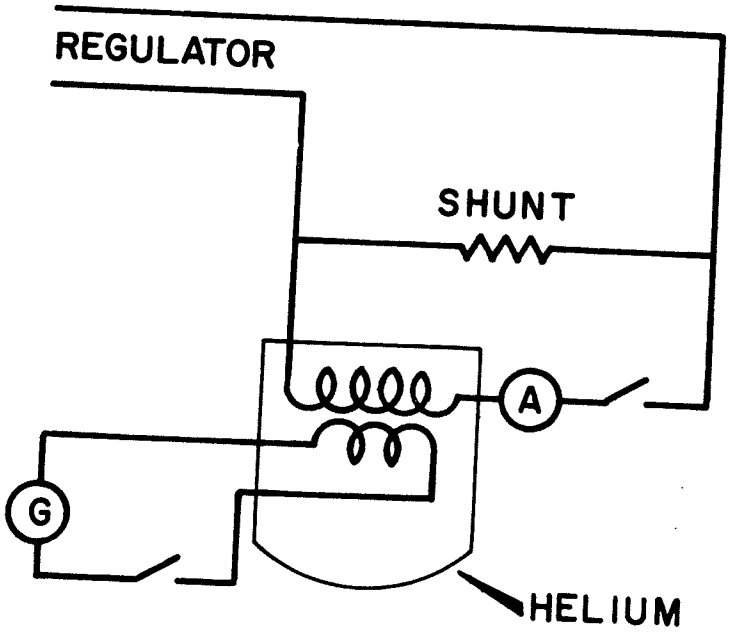

Fig. 19: Diagram of superconducting coil circuit.

calibrated, and the average field obtained by using the deflection-field conversion; from the average field the peak field was easily found. The use of this method was of course limited to situations where the field was either turned on or off. The other method used was to calibrate the coil in the normal state, obtaining a gauss per ampere conversion factor. Since the field equations are dependent only upon the current and the geometry (i.e., independent of the conduction mechanism), this could then be applied directly to find the field for any current in the superconducting state. As the critical current density was reached and the superconducting coil went normal, the field collapsed inside the coil giving a galvenometer deflection, from which the maximum field was calculated. At the same time the current through the coil dropped to essentially zero and a small voltage temporarily appeared across the coil.

The maximum current attainable was substantially below that which had been expected. The current was approximately 80 amperes (current density 6.5×10^4 amperes per square inch), which gave a field of 7.5 kilogauss. Qualitative investigation indicates that the explanation for this lies in the induction of eddy currents within the wires.[27] As the current rises through the superconductor due to external sources, it produces an associated increasing

magnetic field, which in turn gives rise to currents which circulate within a single wire, either parallel to a cross section or back and forth along the wire. This was evidenced by a strong observed residual field, which persisted after the current was switched off manually. If the current was increased past its critical value, the wire would regain its resistivity, and no residual currents were observed. These eddy currents could become quite large, and perhaps the field they produce is sufficient to saturate the superconducting wire and cause it to return to the normal state. It appears that this mechanism increases rapidly with the size of the wire, its ultimate result being that the maximum attainable current density is roughly proportional to the diameter of the wire, and not to the area, as one would probably expect.

Although the results obtained indicated a lower critical current density than expected, the assumptions of current density used in the previous section are consistent with results obtained at other laboratories (see indicated references).

By the time actual construction of such a machine is considered, further developments will undoubtedly allow greater ease in production of such superconductor fields.

REFERENCES

1. L. H. Thomas, Physical Review 54 (1938) 58.

2. E. L. Kelly, R. V. Pyle, R. L. Thornton, J. R. Richardson, B. T. Wright, Review of Scientific Instruments 27 (1956) 493.

3. A. I. Yavin, Physics Today 15 #5 (1962) 19.

4. H. Kamerlingh Onnes, Commun. Phys. Lab. Univ. Leiden (1911) 122b.

5. J. E. Kunzler, E. Buehler, F. S. L. Hsu, J. H. Wernick, Physical Review Letters 6 (1961) 89.

6. J. E. Kunzler & M. Tanenbaum, Scientific American 206 #6 (1962) 60.

7. J. E. Kunzler, Reviews of Modern Physics 33 (1961) 501.

8. Westinghouse descriptive bulletin 45-950, January, 1962.

9. M. M. Gordon & T. A. Welton, Computation Methods for AVF Cyclotron Design Studies, ORNL-2765.

10. W. K. H. Panofsky & M. Phillips, Classical Electricity and Magnetism, Addison-Wesley Publishing Co., Inc., Reading, Mass., 1955.

11. B. T. Smith, Mistic Program for Computation of the Magnetic Field of a Circular Current, MSUCP-8, modified by D. A. Johnson.

12. S. L. Steinberg, Least Squares Code, unpublished.

13. S. L. Steinberg, Fourier Analysis Code, unpublished.

14. T. I. Arnette, Mistic Equilibrium Orbit Code, MSUCP-10.

15. M. M. Gordon & T. A. Welton, op. cit.

16. J. J. Livingood, Cyclic Particle Accelerators, D. Van Nostrand Company, Inc., Princeton, N.J., 1961.

17. K. R. Symon, D. W. Kerst, L. W. Jones, L. J. Laslett, & K. M. Terwilliger, Physical Review 103 (1956) 1837.

18. H. G. Blosser, J. Ballam, G. B. Beard, F. J. Blatt, J. A. Cowen, S. K. Haynes, W. H. Kelly, J. J. LaRue, D. Lichtenberg, R. D. Spence, A. Timnick, Proposal for a Nuclear Research Facility, Document, Physics Department, Michigan State University, 1958, p.55.

19. M. M. Gordon, private communication.

20. The assumed current density was 200,000 amps/in ^{2}, allowing a 25% safety factor. (This is consistent with values given in references 6 and 26).

21. Wah Chang Corporation, Albany, Oregon.

22. R. W. Boom & R. S. Livingston, Proceedings of the IRE Volume 50 No. 3, March, 1962.

23. Bridgeport Insulated Wire Company, Bridgeport, Conn.

24. Emerson & Cummings, Canton, Mass., Eccoseal 1211.

25. R. R. Hake, private communication.

26. R. W. Boom, L. D. Roberts, R. S. Livingston, Developments in Superconductor Solenoids, unpublished.

27. D. B. Montgomery, Current Carrying Capacity of Superconducting Nb-Zr Solenoids AFOSR-3015.